

CHEMISTRY

A European Journal



Accepted Article

Title: Thermally-induced trans-to-cis isomerization and its photo-induced reversal monitored using absorption and luminescence: Cooperative effect of metal coordination and steric substituent

Authors: Minghua Zeng, Jun-Quan Zhang, De-Shan Zhang, Qiu-Jie Chen, Hai-Bing Xu, Mohamedally Kurmoo, and Ming-Hua Zeng

This manuscript has been accepted after peer review and appears as an Accepted Article online prior to editing, proofing, and formal publication of the final Version of Record (VoR). This work is currently citable by using the Digital Object Identifier (DOI) given below. The VoR will be published online in Early View as soon as possible and may be different to this Accepted Article as a result of editing. Readers should obtain the VoR from the journal website shown below when it is published to ensure accuracy of information. The authors are responsible for the content of this Accepted Article.

To be cited as: *Chem. Eur. J.* 10.1002/chem.201900204

Link to VoR: <http://dx.doi.org/10.1002/chem.201900204>

Supported by
ACES

WILEY-VCH

Thermally-induced *trans*-to-*cis* isomerization and its photo-induced reversal monitored using absorption and luminescence: Cooperative effect of metal coordination and steric substituent

Jun-Quan Zhang,^[a] De-Shan Zhang,^[a] Qiu-Jie Chen,^[b] Hai-Bing Xu,^{*[b]} Mohamedally Kurmoo,^[c] Ming-Hua Zeng^{*[a,b]}

Abstract: For ethene derivatives with large groups the *cis*-isomer is often quite unstable and unavailable. Herein, we report an exception of two stable coordination complexes, (*cis*-L)ZnCl₂, starting from *trans*-1,2-bis(1-R-benzo[d]imidazol-2-yl)ethene (R = H, **L1**; R = CH₃, **L2**) ligands under solvothermal condition (T ≥ 140 °C). Using the intensity of the absorption and luminescence spectra as probes we proposed its progressive *cis* to *trans*-reversal upon irradiation with UV light, which was confirmed by PXRD. Similar results observed in the series of (*cis*-L₂)M^{II}Cl₂ (M = Fe (**4**), Co (**5**), Ni (**6**)) demonstrate the universal strategy. The results of PXRD, NMR, ESI-MS and DFT support the above conclusion. NMR indicates irradiation of **1** converts an optimized 71% of the *cis*-isomer to *trans*-one, whereas the free *trans*-L₁ ligand transforms to only 15% *cis*-isomer under similar conditions.

Introduction

Photo-switchable molecules are considered as promising elements in future devices, because their physical and chemical properties, such as absorption spectra, fluorescence, conjugation, coordination, geometrical structure and so on, could be tuned by light during photo-excitation.^[1,2] Till now, there are mainly two homologous photo-switching derivatives with *cis*- / *trans*- isomerization about C=C (stilbene) and N=N (azobenzene) **Scheme 1**.^[3] Due to the significantly higher barrier for thermal isomerization about C=C investigations of stilbene derivatives are less common compared to those of azobenzene ones. Regardless, the progress on photo-isomerization dynamics^[4,5] and the strategy on modulation spectra^[6] of stilbenes derivatives

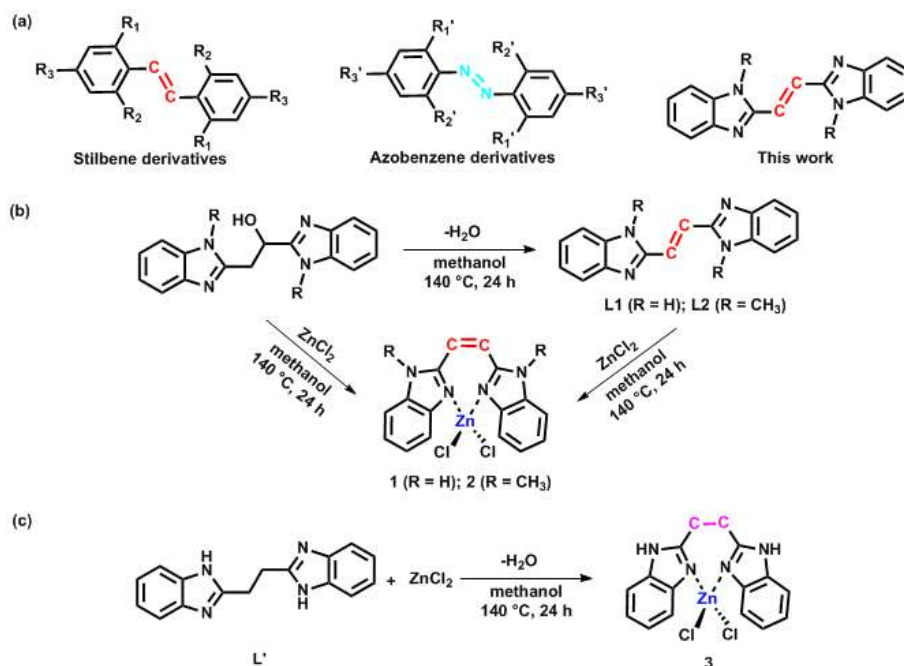
have been revealed. Recently, novel structure and performance of photo-responsive metal compounds (Table S1) have been developed and established.^[7] For instance, McGimpsey used 2,2'-dipyridylethylene ligands to modulate surface wettability by photo-induced *cis*- / *trans*-isomerization.^[8] Employing photo-switchable ligand into a MOF, that undergoes a reversible conformational change upon light exposure, as soft materials are also promising.^[9] Yet the applications especially for the *cis*- / *trans*- isomerization about C=C bonds are limited somewhat by two intrinsic drawbacks: 1) information on the *cis*-isomer remains insufficient in most cases, due to their instability,^[2,6] and 2) although the spectra could be modulated by substitution at corresponding position, the spectral change for *cis*- and *trans*-isomers is subtle,^[10] severely limiting their developments.

It has been established by a combination of X-ray crystallography and mass spectrometry (MS), the mechanisms of the formation of polyoxometalate clusters,^[11] coordination cages,^[12] and 3d-metal clusters^[13,14] could be successfully unveiled. Recently, combination magnetic resonance spectroscopy (NMR), followed by the former two techniques, a plausible reaction mechanism of an Fe²⁺-catalyzed domino *in situ* N-alkylation reaction of 2-(Hydroxymethylhydroxymethyl) quinoline-8-ol (HL-OH) with NEt₃ / NH₃ for a trinuclear iron cluster [Fe₃(L₃-N)₂] were proposed.^[15] Furthermore, utilizing the former two techniques and isotope labeling, a longest domino reaction involves 14 steps and the formation of 12 covalent bonds and 3 heterocycles of a new type of triheteroarylmethyl radical had been clearly unraveled.^[16] Encouraged by these successes, we want to deduce the possible structures of *cis*- / *trans*-isomers of photo-responsive metal compounds under photoexcitation by single crystal and powder crystallography, ESI-MS, and NMR.

To the best of our knowledge, stabilizing *cis*-isomer by chelating metal ion with photo-switching *trans*-molecules, and improving photo-isomerization efficiency has yet to be reported. Herein, stable (*cis*-L)ZnCl₂ (**L1**, **1**; **L2**, **2**) were afforded by chelating ZnCl₂ starting with *trans*-1,2-bis(1-R-benzo[d]imidazol-2-yl)ethene (R = H, **L1**; R = CH₃, **L2**), and it was found that 71% *cis*-configuration could convert into *trans*-one for **1**, while only 15% of pure *trans*-L₁ transforms into *cis*-isomer during irradiation. Although, subtle changes of spectra present in both **L1** and **L2**, markedly intensity enhancement in both absorption and emission of **1** and **2** are observed during irradiation within second scale. Similar results of a comparative study on a series of (*cis*-L₂)M^{II}Cl₂ (M = Fe (**4**), Co (**5**), Ni (**6**)) verify the strategy is universal. Through the coincident results of crystallography, ESI-MS, NMR, PXRD, and DFT, we deduced the configurational transition of **1** during photo-isomerization.

- [a] J.-Q. Zhang, D.-S. Zhang, Prof. Dr. M.-H. Zeng
Key Laboratory for the Chemistry and Molecular Engineering of Medicinal Resources, School of Chemistry and Pharmaceutical Sciences, Guangxi Normal University, Guilin, 541004, P. R. China.
E-mail: zmh@mailbox.gxnu.edu.cn
- [b] Q.-J. Chen, Prof. Dr. H.-B. Xu, Prof. Dr. M.-H. Zeng
Key Laboratory for the Synthesis and Application of Organic Functional Molecules, College of Chemistry and Chemical Engineering, Hubei University, Wuhan 430062, P. R. China.
E-mail: xhb@hubu.edu.cn
- [c] Dr. M. Kurmoo
Université de Strasbourg, Institut de Chimie de Strasbourg, CNRS-UMR7177, 4 rue Blaise Pascal, Strasbourg Cedex 67070, France.

Supporting information for this article is available on the WWW under <http://dx.doi.org/10.1002/chem.2019xxxxx>



Scheme 1. (a) Photo-isomerization of photo-switches through double bonds (the functional group on the phenyl rings may be the same or different); (b) Synthetic procedures of **L1** / **L2** and metal compounds **1–2**; (c) Synthetic procedure of reference compound **3**; (H atoms of carbon are omitted for clarity).

Results and Discussion

Although **L1** and **1** had been characterized previously (Table S1),^[17] the reported spectral properties were preliminary and of low resolution. The temporal effect of irradiation was not studied and photo-induced isomerization for both **L1** and **1** not reported. Given the principle of orbital symmetry conservation, the photo-cycloaddition^[18] in relatively concentrated solutions were also not discussed.

Syntheses

In-situ solvothermal reaction at 140 °C for 24 hours led to the dehydration of 1,2-bis(1-R-benzo[d]imidazol-2-yl)ethanol in methanol to exclusively *trans*-1,2-bis(1-R-benzo[d]imidazol-2-yl)ethene [R = H, **L1**; R = CH₃, **L2**] as pale yellow block crystals (**Scheme 1**). While their reactions with ZnCl₂ led to the (*cis*-L)ZnCl₂ compounds (**L1**, **1**; **L2**, **2**). The metal complexes were also obtained in a one-pot reaction of ZnCl₂ with 1,2-bis(R-benzo[d]imidazol-2-yl)ethanol. It appears that through the slow *in-situ* dehydration the target crystals suitable for X-ray diffraction were formed. To get a deeper insight into the reaction procedure, we synthesize *trans*-L to react with ZnCl₂ under the same condition, also achieving (*cis*-L)ZnCl₂, the productivity based on **L1** and **L2** is higher than that of the former. In parallel, a series of (*cis*-L₂)M^{II}Cl₂ (M = Fe (**4**), Co (**5**), Ni (**6**)) were synthesized under the same conditions.

To verify whether photo-isomerization and photo-cycloaddition reactions may occur during the syntheses of compounds **1** and **2** by irradiation, an analog ligand with C-C single bond bridging two benzo[d]imidazole, 1,2-bis(1H-benzo[d]imidazol-2-yl)ethane (**L'**) was used to make the corresponding L'ZnCl₂ (**3**) as reference.

Crystal Structures

The compounds were all characterized by elemental analyses, IR spectroscopy, TG, PXRD, ESI-MS, ¹H-NMR, and X-ray crystallography. The crystallographic data of **L1**, **L2**, **1**, **2**, **L'** and **3–6** are summarized in Table S2. Selected atomic distances and angles for **1–3** are presented in Table 1. The crystal structures are depicted in Figure 1.

The crystal structures of **L1** and **L2** are similar to that of **L'** (Figure 1). They can be viewed as two benzo[d]imidazole separated by C=C for **L1** and **L2** and C–C for **L'** in a symmetric *trans*-configuration. The C–C bond multiplicities were confirmed by the bond lengths of C8–C8a (1.338 Å) of **L1** and **L2** being shorter than that of **L'** (1.501 Å). Due to the steric hindrance from –CH₃ of imidazole groups, the angle of C7–C8–C8a in **L2** (123.8°) is slightly smaller than that in **L1** (125.2°), but all much larger than that in **L'** (113.0°).

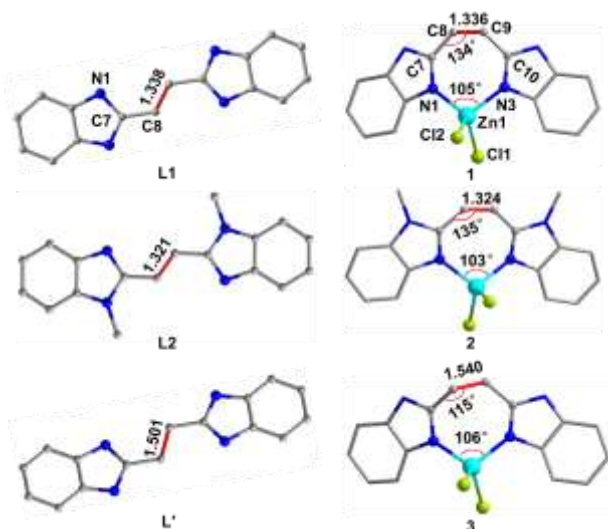


Figure 1. Crystal structures of **L1**, **L2**, **L'** and compounds **1–3**. (H atoms are omitted for clarity).

Similarly, the crystal structures of **1** and **2** resemble that of **3**, in which the Zn^{2+} exhibits distorted tetrahedral coordination with two N atoms from a chelating *cis*-configured ligand and two terminal Cl ions. The C7–C8 bond lengths of 1.452 Å in **1**, and 1.441 Å in **2** and C9–C10 of 1.450 Å in **1**, and 1.441 Å in **2** are shorter than those in **3** (1.502 Å and 1.503 Å). The bond lengths of Zn1–Cl1 (2.281 Å in **1**, and 2.305 Å in **2**) and Zn1–Cl2 (2.229 Å in **1**, and 2.231 Å in **2**) are different where Zn1–Cl1 is longer than Zn1–Cl2, but in **3** they are similar (2.250 Å and 2.253 Å, respectively). Due to double bond (C=C) between two benzo[d]imidazole in both **1** and **2**, the bond lengths of C8=C9 (1.336 Å in **1**, and 1.323 Å in **2**) are much shorter than that in **3** with single bond (1.539 Å). However, the angles of C7–C8=C9 (134.0° in **1**, and 135.5° in **2**), C8=C9=C10 (134.8° in **1**, and 135.1° in **2**) are much larger than those in **3** (115.2° and 115.1°, respectively). It is interesting to note that the angles of N1–Zn1–N3 in **1** (105.1°) and **2** (103.2°) are smaller than that in **3** (106.4°), indicating potential energy within the structure of **1** and **2**.

Table 1. Selected Bond Lengths (Å) and Angles (°) for **L**, **1**, **2**, **L'**, and **3**.

Bonds and Angles	1	2	3
C7–C8	1.452(1)	1.441(7)	1.502(7)
C8–C9	1.336(1)	1.323(7)	1.539(7)
C9–C10	1.450(1)	1.441(6)	1.503(7)
Zn1–Cl1	2.281(2)	2.305(4)	2.250(4)
Zn1–Cl2	2.229(2)	2.231(2)	2.253(6)
N1–Zn1–N3	105.1(3)	103.2(2)	106.4(0)
Cl1–Zn1–Cl2	105.1(5)	113.5(9)	111.0(9)
C7–C8–C9	134.0(8)	135.5(4)	115.2(4)
C8–C9–C10	134.8(8)	135.5(4)	115.2(4)
	L1 (R = H)	L2 (R = CH₃)	L'
C8–C8a	1.338(3)	1.321(4)	1.501(4)
C8a–C8–C7	125.2(4)	123.8(2)	113.0(2)

Symmetry code: (a) $-x+1, -y, -z+1$.

Photophysical properties

UV-Vis absorption spectra of **L1**, **L2**, **L'** and **1–3** in DMSO are shown in Figure 2, and their molar absorption coefficients are listed in Table S3. Due to electron-donating effect of the methyl in **L2**, the maximal absorptions show slight bathochromic shifts to 378 nm extending to 420 nm from 364 nm reaching to 400 nm for **L1**. As for inferior conjugacy of **L'**, significant hypsochromic shifts to 284 nm trailing to 300 nm is observed.

From the DFT calculations (Table S4), the absorption bands from 200 to 400 nm are assigned as π – π and n– π transitions. Since different symmetries of the *cis*- and *trans*-isomers for **L1** and **L2**, superior π – π stacking among *trans*-isomer to that of *cis*-one induces redshift of absorption bands, which is also confirmed by the steric hindrance from two benzo[d]imidazo groups in the structure of *cis*-isomer. Additionally, the more π – π stacking interactions the higher transition probability induce enhancement on absorption intensity, thus the intensity of *trans*-isomer is higher than that of the *cis*-one.

After coordination with $ZnCl_2$, similar absorption bands ascribed to the intraligand transitions appear, since the corresponding bands are found for the free ligands. However, the molar absorption coefficients of **1** and **2** are much lower than those of the free ligands **L1** and **L2** (Table S3), because of their different configurations in *trans*-L and (*cis*-L) $ZnCl_2$.

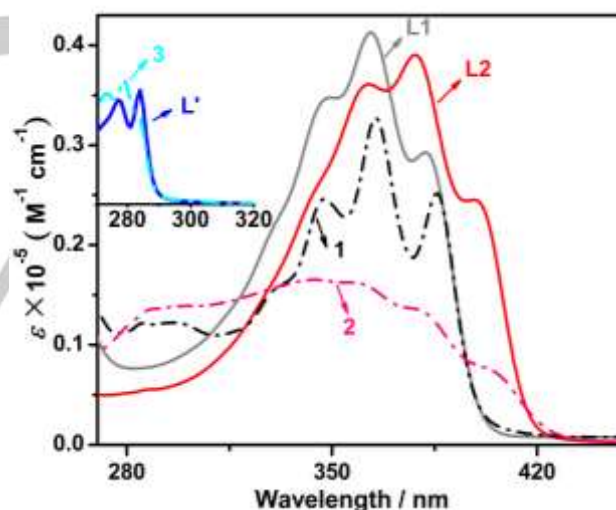


Figure 2. UV-Vis absorption spectra of ligands and corresponding metal compounds in DMSO.

The absorption spectra of the ligands and metal complexes are characterized by a band centered at ca. 370 nm which exhibits a vibrational progression with an average separation of 1300 cm^{-1} . While the resolution appears to increase for **1** compared to **L1**, it is reduced from **L2** to **2**. The intensities of the band for the metal complexes are less intense compared to the corresponding ligands. Interestingly, upon irradiation with two 18-Watt 365 nm UV lamps, the absorption band intensities of the UV-Vis spectra are marginally lowered for both **L1** (0.98 times, Figure S5a) and **L2** (0.91 times, Figure S5c). In contrast, the absorption

intensities of (*cis-L*)ZnCl₂ increase markedly during irradiation within timescale of seconds (Figure 3). For **2**, the absorption bands gradually become clear and discernable, finally like the profile of **L2**, and 2.60 times of absorption intensity enhancement could be induced within 15 seconds (Figure S5d). In parallel, only 1.22 times of absorption intensity enhancement could be attained within 27 seconds for **1** under the same condition (Figure S5b). All the facts, on the one hand, suggest large enhancement on absorption intensity could be afforded in (*cis-L*)ZnCl₂ by chelation metallic ion, thus the absorption intensity enhancement for **2**

(2.60 times) and **1** (1.22 times) is more obvious than those attentions of **L2** (0.91 times) and **L1** (0.98 times). On the other hand, steric substitution in the ortho-position also benefit for improving spectral intensity, inducing larger enhancement for **2** than that for **1**. Finally, as discussed in the crystal structure section, the potential energy within the structure contributes for photo-isomerization, inducing the faster rate for **2** (15 seconds) than for **1** (27 seconds). Consequently, due to lacking photo-isomerization, negligible changes of absorption intensity in both **L'** (Figure S5e) and **3** (Figure S5f) could be observed.

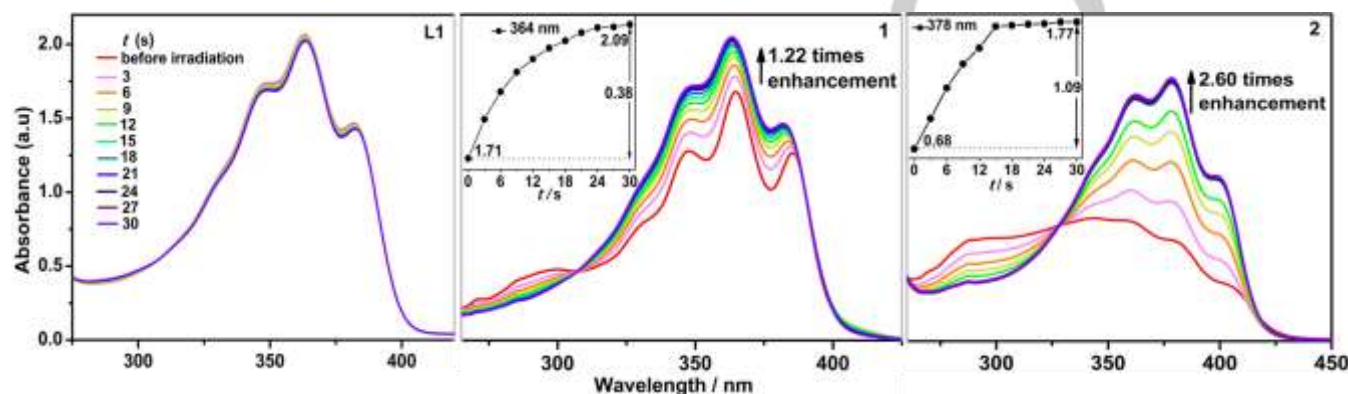


Figure 3. Absorption intensity enhancement of **L1**, **1** and **2** in DMSO during irradiation with 365 nm.

Upon excitation, bright blue luminescence centered at ca. 420 nm for **L1** (Figure S6a), 442 nm for **L2** (Figure S6c), and 406 nm for **L'** in DMSO (Figure S6e) occurs. Although negligible emission changes during irradiation is observed for all of them, significant emission enhancement is found by chelating them with metallic ion to afford (*cis-L*)ZnCl₂ under the same condition. Since the substituents on the imidazole nitrogen for **2** (-CH₃) is bulkier than that for **1** (-H), emission increment for **2** (5.10 times, Figure S6d)

is larger than that of **1** (2.75 times, Figure S6b) during irradiation. Noteworthy, the emission enhancement of **2** (2.3 times) is much faster than that of **1** (1.6 times) within the first three seconds (Figure 4). Moreover, after **1** in DMSO was excited at 365 nm for 30 seconds, the absorption and emission intensities almost remain unchanged under dark environment for 12 and 24 hours (Figure S7), indicating the photo-isomerization procedure is irreversible.

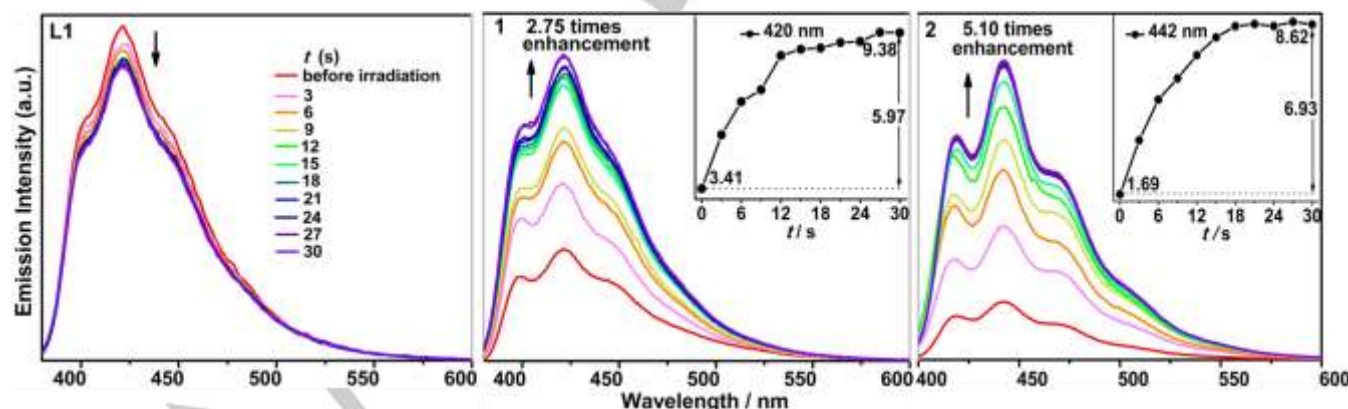


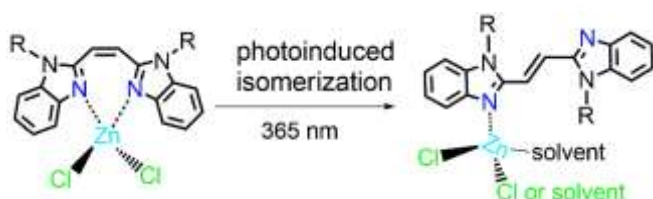
Figure 4. Emission intensity enhancement of **L1**, **1** and **2** in DMSO during irradiation.

In order to verify the universal strategy, we synthesize and performed a comparative study of a series of (*cis-L2*)M^{II}Cl₂ (M = Zn (**2**), Fe (**4**), Co (**5**), Ni (**6**)). From their crystal structures (Figure

S1), the bond lengths of C8=C9 vary from 1.330 Å in (*cis-L2*)NiCl₂ to 1.338 Å in (*cis-L2*)FeCl₂, and the angles of N1-M-N3 are from 98.1° in (*cis-L2*)FeCl₂ to 103.2° in (*cis-L2*)CoCl₂

(Table S5). Correspondingly, the absorption intensity enhancements are from 1.60 times for (*cis*-L2)FeCl₂ (Figure S8a) to 2.30 times for (*cis*-L2)NiCl₂ (Figure S8c), and the ones of luminescence are from 2.29 times for (*cis*-L2)NiCl₂ (Figure S8c) to 6.54 times for (*cis*-L2)FeCl₂ (Figure S8a) during irradiation (Table S6). The take away information photoinduced *cis* / *trans*-isomerization through C=C bonds can be regulated incorporating steric substituents and coordination to metallic ions (Figures 3-4).

Additionally, after irradiation of the metal compounds **1** and **2** for a long time (24 hours), their absorption spectra could not overlap completely with those of free L1 and L2 (Figure S9), respectively, indicating *cis*-configurational metal compounds could not completely convert into *trans*-isomers. With reference to the photo-induced *cis*-/*trans*- isomerization structures of 2,2'-dipyridylethylene Cu^{II} compound,^[8] we may deduce that the Zn²⁺ chelating with *cis*-L converts into Zn²⁺ bridging with *trans*-L during photo-isomerization as Scheme 2. Further to confirm it, we react ZnCl₂ with L1 and 1,2-bis(1-R-benzo[d]imidazol-2-yl) ethanol by solvothermal reaction in methanol at 130 °C instead of 140 °C for 24 hours, it was found that **1** could not be obtained as verified by the PXRD (Figure S11). This sets the barrier energy required to convert *trans* to *cis* for chelation with the Zn²⁺ to *kT* (T = 140 °C). On the other hand, mixture of ZnCl₂ with L1 / L2 in DMSO, there are some downfield shifts in the ¹H-NMR spectra compared to that of free L1 / L2 (Figures S12a and S12b), suggesting the ZnCl₂ bridges with L1 / L2 as shown in Scheme 2.



Scheme 2. Possible structures of (*cis*-L)ZnCl₂ under photo-isomerization in DMSO.

On the question of reversibility, we examine the crystal phases using powder diffraction due to the lack of single crystals from reactions of ZnCl₂ with the *trans*-L1 at temperature less than 140 °C. For reactions at 25 °C and those treated solvothermally up to 130 °C (Figure 5), the strikingly similar patterns with different intensity suggest the same compound is formed. While the pattern changed when the temperature is set at 140 °C and it corresponds to that simulated from the crystal data of (*cis*-L1)ZnCl₂. The pattern for the irradiated (*cis*-L1)ZnCl₂ in DMSO for 6 hours followed by evaporation to dryness in air was the same as those of the powders obtained up to 130 °C without any Bragg reflection originating from the (*cis*-L1)ZnCl₂. All these facts further confirm the transformation of (*cis*-L1)ZnCl₂ by irradiation and reversal of the ligand conformation from *cis* to *trans* as suggested in Scheme 2.

Given the possibility of photo-cycloaddition^[18] instead of photo-isomerization,^[12] where the former effect is expected to blue shift the absorption and emission energies due to removal

of the conjugation, the latter can have little difference, we studied the reference compound **3** which has a C-C single bond center to obtain the reference point in spectral energy (Figure S13). The small energy shifts in the spectra of **1** and **2** (Figures S5b-S5d) therefore suggests there is no photocycloaddition (Figures 2 and 3). Thus, the change in spectral intensity is associated with photoinduced isomerization.

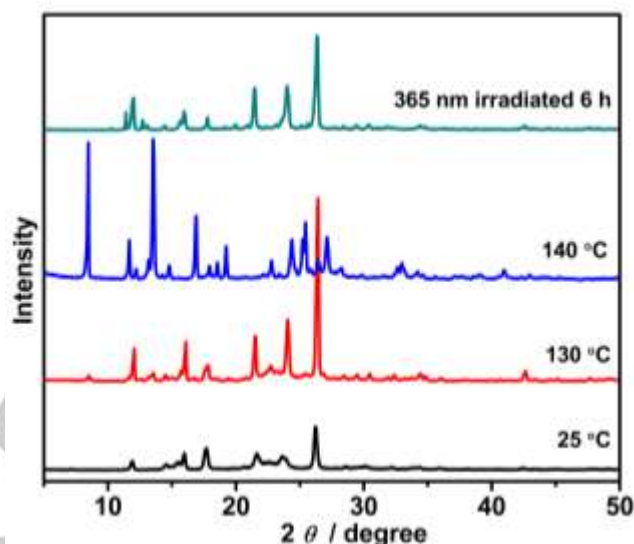


Figure 5. The PXRD patterns of the reaction products of ZnCl₂ with L1 in methanol at 25 °C (black), solvothermal at 130 °C (red) and 140 °C (blue) for 24 hours, and the one of the irradiated **1** in DMSO for 6 hours followed by evaporation to dryness in air (dark cyan).

Configurational transitions of photo-isomerization by ESI-MS

Due to higher solubility of **1** than **2**, we dissolve the crystals of **1** in DMSO and diluted with CH₃OH and collected MS under different in-source energies (Figures 6a and S14), it was found that three single series of peaks in the positive mode spectra at *m/z* 261.11 [L1 + H]⁺, 359.00 [L1 - Cl]⁺, and 437.02 [L1 + DMSO - Cl]⁺ appear until the in-source energy reached 60 eV, suggesting the integrity of the cores of **1** is stable.

The photo-isomerization process of **1** monitored by ESI-MS under irradiation (Figures 6b and S15) with two 18-Watt 365 nm UV lamps within various times were performed. Three peaks in the positive mode spectra of [L1+(Solvent)₂-Cl]⁺ (Solv = DMSO + H₂O, 455.03; DMSO + CH₃OH, 469.04; 2DMSO, 515.03), beside three peaks at 261.11, 359.00 and 437.02 as previous experiment, are observed. The results together with the abundance of fragment [L1+(Solvent)₂-Cl]⁺ increasing with the irradiation time (Figures 6c), indicate the (*cis*-L1)ZnCl₂ activated by irradiation transfers into *trans*-one, favoring for the more solvent molecules (including DMSO / H₂O / CH₃OH) coordination with Zn²⁺ (as suggest in Scheme 2).

As for L1 under the same condition, no new peaks especially of dimer signals of photocycloaddition product in the positive

mode spectra (Figure S15a) could be observed during irradiation, indicating photocycloaddition reaction does not happen in **L1**.

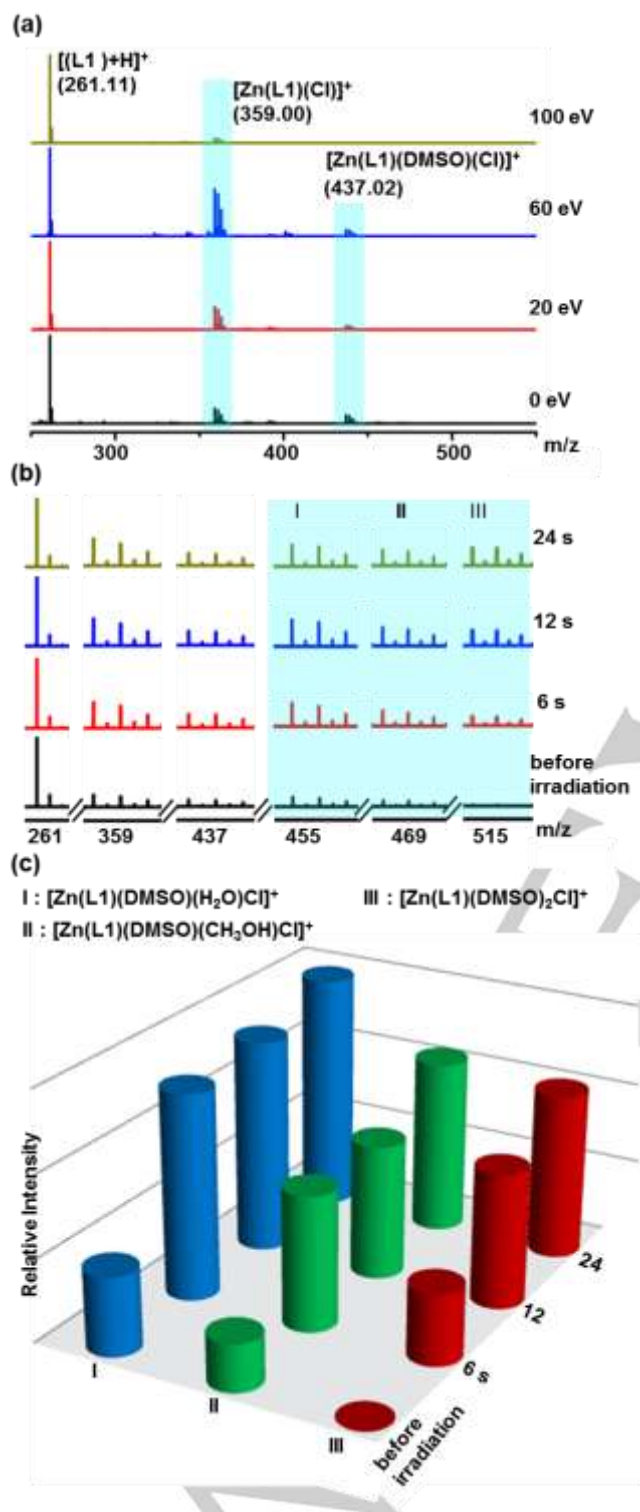


Figure 6. Positive mode ESI-MS spectra of crystal of **1** dissolved in DMSO/CH₃OH under various in-source energies (a) and after irradiation for various times (b), the peak intensity in the region of m/z 455.03 and 469.04 have been amplified for clarity, and the abundance of fragment [1+(Solv)₂-Cl]⁺ increasing with the irradiation time (c).

Density Functional Theory Calculations (DFT)

According to the typical composition of peaks of the MS spectra, the possible structures of fragments are fully optimized and their corresponding Gibbs free energies (Figure S16) were calculated. As revealed from the calculated coordination energies, changing from *trans*-**L1** to *cis*-**L1** is easier than to intermolecular [2 + 2] photocycloaddition product, because two C=C bonds need to be broken into two C-C bonds with bonding energy as high as 162 kcal/mol, beside the energy to surmount the steric hindrance. In parallel, transforming *cis*-**1** into *trans*-**1** with Zn-N broken is more feasible than intermolecular [2 + 2] photocycloaddition of the metal compound. As for **2**, the former transformation instead of the latter one is more workable than those of **1**, as the bulky substituent contributes to isomerization, but impedes dimerization by steric hindrance. Thus, DFT calculations indicate Zn²⁺ coordination to *trans*-L is more favorable than with *cis*-L. With irradiation the *cis*-L is more easily transformed into *trans*-L. Consequently, the energetics favor Zn²⁺ bridging with *trans*-L (Scheme 2). All the results are coincident with the suggestion of the ESI-MS.

Conversion efficiency of photo-isomerization by ¹H-NMR

In order to verify the conversion efficiency during photo-isomerization reaction, the ¹H-NMR measurements were carried out to monitor the configuration changes during irradiation for 0.5 h with 365 nm. Before irradiation, **L1** in DMSO-*d*₆ at 298 K exhibits four distinguishable proton signals at 12.93, 7.63, 7.60, and 7.23 ppm (Figure 7a), ascribed respectively to (a) two H on the nitrogen atoms in imidazole, (b) two H on the C=C, (c) four H on the benzene near the imidazole, and (d) four H on the benzene opposite the imidazole. After coordination with ZnCl₂ to form (*cis*-**L1**)ZnCl₂, we can clearly detect the proton signals of two H on the C=C in *cis*-isomer of **1** up-field to 7.18 from 7.63 in *trans*-**L1** (Figure 7c). Upon irradiation of *trans*-**L1** for 0.5 h with two 18-Watt 365 nm UV lamps, three sets of proton signals at 7.85, 7.35 and 7.05 ppm ascribed to the typical *cis*-isomer appear besides those of the *trans*-**L1** (Figure 7b), manifesting the formation of *cis*-**L1** in NMR time scale. Similarly, irradiation of **1** for 0.5 h, three sets of proton signals at 7.24, 7.62 and 7.68 ppm ascribed to the typical *trans*-isomer like *trans*-**L1** appear besides those of the (*cis*-**L1**)ZnCl₂ (Figure 7d). From the changes of the proton peak area, we can clearly detect ca. 15% *trans*-**L1** transformation into *cis*-**L1**, and 71% conversion of coordinated *cis*-L of **1** to *trans*-L during photo-isomerization reaction.

Although the solubility of **2** and **L2** is poorer than that **1** and **L1** in DMSO, the ¹H-NMR measurements of **L2** and **2** (Figure S17) with weak signals under the same condition were also carried out. It was found that there are almost no changes for *trans*-**L2** before and after irradiation, while five sets of proton signals at 7.95, 7.69-7.67, 7.63-7.62, 7.31-7.25 and 4.03 ppm ascribed to the typical *trans*-configuration, like those of *trans*-**L2**, appeared besides those of *cis*-one for **2**. These facts indicate that *trans*-**L2** is too stable to transform into *cis*-**L2**, and it is feasible to stabilize (*cis*-**L2**)ZnCl₂ (**2**) by chelating Zn²⁺ with *trans*-**L2**, the quantum yields for *cis* → *trans* is ca. 34%. Due to the steric hindrance from

the two $-CH_3$ of **L2**, it is necessary to overcome larger energy for **L2** than that for **L1**, confirmed by the DFT calculations, to transfer into *cis*-isomer, thus the photo-isomerization of **L1** is more obvious than that of **L2**. On the other hand, as discussed in crystal structure, although the potential energy within the

structure, which would benefit for improving the *cis* \rightarrow *trans* conversion by energy releasing, the steric hindrance from the two $-CH_3$ of **2** inhibits the *cis* \rightarrow *trans* conversion, thus the conversion efficiency of **2** (34%) is lower than that of **1** (71%).

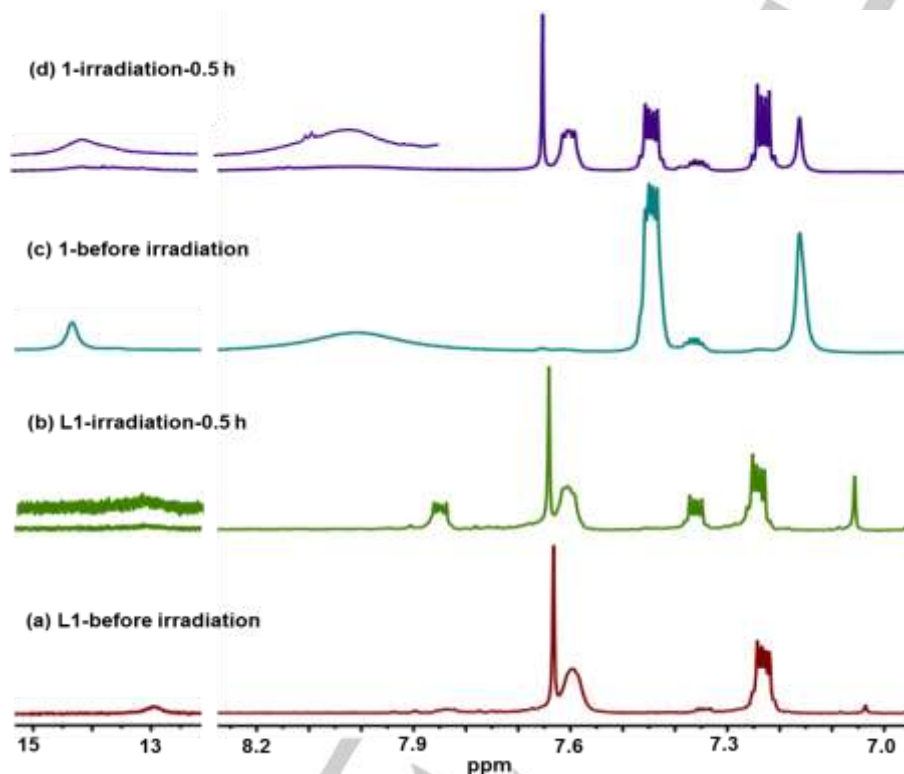


Figure 7. $^1\text{H-NMR}$ spectra of **L1** and **1** before and after irradiation for 0.5 hour.

Conclusions

While *trans*-1,2-bis(1-*R*-benzo[d]imidazol-2-yl)ethene ($R = \text{H}$, **L1**; $R = \text{CH}_3$, **L2**) are sterically more stable than their *cis*-isomers, thermal treatments at $T \geq 140$ °C (isomerization barrier energy) of the *trans*-isomers in the presence of divalent metal halides ($M = \text{Fe}$, Co , Ni , Zn) crystallize (*cis*-**L**) MCl_2 in preference. The photo-excitation at 365 nm of the complexes progressively transform the chelated *cis*-isomer ligand to its *trans*-isomer in a time scale of less than one minute. Due to the difference of the intensities of the UV-Vis absorption and luminescence of the two isomers (*trans* > *cis*), it was used to monitor the progress of the transformation. PXRD and NMR suggest the ligand remains coordinated after photoinduced isomerization and irradiation reverses the ligand configuration from *cis* back to *trans*. Steric substituent on the ligand also affects the intensities and rate. Combining the results of ESI-MS, NMR, PXRD, and DFT, we infer that the metallic ions are possibly bridged by *trans*-**L** instead of chelated by the *cis*-**L** following irradiation. This strategy of trapping the unstable isomer by coordination may be used in

developing new member of photo-responsive coordination compounds.

Experimental Section

Trans-1,2-di(1H-benzo[d]imidazol-2-yl)ethene (L1). Benzene-1,2-diamine (15.14 g, 140 mmol) and fumaric acid (8.12 g, 70 mmol) were dissolved in 100 mL 4 M hydrochloric acid. The solution was heated to reflux for 24 hours where it changed to green-yellow. After cooling, it was neutralized with ammonia to give a yellow precipitate which was filtered. The powder was recrystallized from 250 mL 4 : 1 ethanol-water followed by filtering, washing and drying. Yield 9.50 g (52%). Selected IR (KBr): 2746 (m), 1590 (w), 1529 (w), 1426 (s), 1322 (m), 1235 (m), 1148 (m), 1034 (m), 973 (m), 870 (m), 745 (s) cm^{-1} . $^1\text{H-NMR}$ (400 MHz, DMSO-d_6): δ 12.88 (s, 2H), 7.63 (s, 2H), 7.66 (d, $J = 7.8$ Hz, 2H), 7.52 (d, $J = 7.8$ Hz, 2H), 7.25 (t, $J = 7.3$ Hz, 2H), 7.20 (t, $J = 7.6$ Hz, 2H). ESI-MS: $m/z = 261$ [$\text{C}_{16}\text{H}_{12}\text{N}_4 + \text{H}$] $^+$.

Trans-1,2-di(1-methyl-1H-benzo[d]imidazol-2-yl)ethene (L2). *N*-Methyl-1,2-phenylene diamine (27.3 g, 140 mmol) and fumaric acid (8.12 g, 70 mmol) were dissolved in 150 ml 4 M hydrochloric acid. The solution was heated to reflux for 24 hours. After cooling, a green

compound crystallized from the brown solution. The powder was filtered and dissolved in 500 mL 4:1 ethanol–water. After adding active carbon, the solution was heated to reflux for 10 minutes. The green solution was neutralized with ammonia giving a yellow precipitate which was filtered, washed and dried. Yield 5.25 g (25%). Selected IR (KBr): 3067 (w), 2956 (w), 1602(w), 1471 (s), 1346 (s), 1405(m), 1306 (m), 1238 (m), 923 (m), 854 (m), 751 (s), 563 (m) cm^{-1} . ESI-MS: $m/z = 289$ [$\text{C}_{18}\text{H}_{16}\text{N}_4 + \text{H}$] $^+$.

1,2-di(1*H*-benzo[*d*]imidazol-2-yl)ethane (L¹). Benzene-1,2-diamine (15.14 g, 140 mmol) and succinic acid (8.26 g, 70 mmol) were dissolved in 100 mL 4 M hydrochloric acid. The solution was heated to reflux for 24 hours to a faint yellow color. After cooling, it was neutralized with ammonia and the yellow precipitate was filtered. The powder was recrystallized in 300 mL 4 : 1 ethanol–water. After cooling, the white precipitate was filtered, washed and dried. The yield of L¹ was 11.25 g (61%). Selected IR (KBr): 2744 (s), 1625 (w), 1541 (m), 1435 (s), 1319 (w), 1268 (m), 1221 (m), 1032 (m), 911 (m), 870 (m), 740 (s) cm^{-1} . ¹H NMR (400 MHz, DMSO-*d*₆): $\delta = 7.85$ (m, 4H, ArH), 7.65 (m, 4H, ArH) and 3.82 (s, 4H, CH₂). ESI-MS: $m/z = 263$ [$\text{C}_{18}\text{H}_{14}\text{N}_4 + \text{H}$] $^+$.

Synthesis of metal compounds (1-3). A mixture of ZnCl₂ (1.0 mmol, 0.14 g), L¹ (1.0 mmol, 0.28 g) / L² (1 mmol, 0.31 g) / L¹ (1 mmol, 0.26 g) and methanol (15 mL) was sealed in a 25 mL Teflon-lined steel autoclave and heated at 140 °C for 24 h. After the autoclave was cooled to room temperature at a rate of 10 °C min⁻¹, light yellow block crystals of the metal compounds (1-3) were obtained. The absence of solvent was confirmed by thermogravimetric and elemental analyses (EA). Phase purity was confirmed by PXRD (Fig. S4).

1. Anal. Calcd for Zn(C₁₆H₁₂N₄)Cl₂: C 48.46, H 3.56 and N 14.13. Found (%): C 48.32, H 3.69, and N 14.09. Selected IR (KBr): 3221 (s), 1590 (w), 1457 (m), 1349 (m), 1230 (w), 1146 (w), 1042 (m), 805 (m), 749 (s), 587 (m). Yield, 55 mg, 14% based on L¹.

2. Anal. Calcd for Zn(C₁₈H₁₆N₄)Cl₂: C 50.91, H 3.80, and N 13.19. Found (%): C 50.85, H 3.77 and N 13.25. Selected IR (KBr): 3068 (w), 2957 (w), 1593 (w), 1470 (s), 1339 (m), 1240 (m), 1146 (w), 1018(w), 918 (w), 857 (w), 748 (s), 559 (w). Yield, 80 mg, 19% based on L².

3. Anal. Calcd for Zn(C₁₆H₁₄N₄)Cl₂: C 48.21, H 3.54 and N 14.06. Found (%): C 48.32, H 3.63, and N 14.17. Selected IR (KBr): 3289 (s), 3196 (s), 1620 (w), 1542 (m), 1462 (s), 1340 (m), 1279 (m), 1208 (m), 1060 (s), 552 (m). Yield: 45 mg, 23% based on L¹.

4. Anal. Calcd for Fe(C₁₆H₁₄N₄)Cl₂: C 52.08, H 3.89 and N 13.50. Found (%): C 51.92, H 4.01, and N 13.27. Selected IR (KBr): 3078 (w), 2954 (w), 1602 (w), 1474 (s), 1366 (m), 1341 (m), 1307 (m), 1239 (m), 1151 (m), 858(m), 753 (s), 558 (w). Yield: 115 mg, 28% based on L².

5. Anal. Calcd for Co(C₁₆H₁₄N₄)Cl₂: C 51.70, H 3.86 and N 13.40. Found (%): C 51.12, H 3.99, and N 13.68. Selected IR (KBr): 3058 (w), 2945 (w), 1602 (w), 1466 (s), 1342 (s), 1307 (m), 1243 (m), 1154 (w), 851(m), 756 (s), 537 (w). Yield: 178 mg, 43% based on L².

6. Anal. Calcd for Ni(C₁₆H₁₄N₄)Cl₂: C 51.73, H 3.86 and N 13.41. Found (%): C 51.27, H 4.11, and N 13.13. Selected IR (KBr): 3068 (w), 2944 (w), 1593 (w), 1470 (s), 1336 (m), 1341 (m), 1303 (w), 1236 (m), 1156 (m), 858(m), 753 (s), 564 (w). Yield: 205 mg, 49% based on L².

Materials and methods

All chemicals were obtained from commercial sources and used as received without further purification. Elemental analyses for C, H, and N

were performed using Vario Micro Cube. Thermogravimetric analyses (TGA) were performed in a flow of nitrogen at a heating rate of 5 °C min⁻¹ using a NETZSCH TG 209 F3. Infrared spectra of compounds were obtained by transmission through KBr pellets containing ca. 0.5% of the compound using a PE Spectrum FTIR spectrometer (400–4000 cm^{-1}). Powder X-ray diffraction (PXRD) intensities were measured at 296 K using a Rigaku D/max-III A diffractometer (Cu K α). The crystalline powder sample was prepared by crushing the crystals, and scans of 5–60° were conducted at a rate of 5° min⁻¹. The calculated diffraction patterns of the compounds were generated using the Mercury 3.0 software. A THERMO Finnigan LCQ Advantage Max ion trap mass spectrometer was used to collect ESI-MS spectra. A Perkin-Elmer Lambda 35 spectrometer was used to measure the UV-Vis absorption spectra of ligands and compounds. The emission luminescence and lifetime properties were recorded with an Edinburgh FLS 920 fluorescence spectrometer.

X-ray Crystallography. Single-crystal X-ray diffraction data for L¹, L² and L¹ and 1–6 were collected on a Rigaku R-AXIS SPIDER IP diffractometer employing graphite-monochromated Cu-K α radiation ($\lambda = 1.54184$ Å) using the θ - ω scan technique at 150 K. Their structures were solved by direct methods using *ShelXS* and refined using full matrix least-squares technique within *ShelXL2015* and *OLEX.2*.^[19] All non-hydrogen atoms were refined with anisotropic thermal factors. Because of the noncentrosymmetric space group and a Flack parameter about 0.5 of 1 and 3 an absolute structure refinement was performed using the SHELX-2015 TWIN instruction.^[20] Crystallographic data have been deposited at the Cambridge Crystallographic Data Center. The crystallographic data (CCDC-1887730, 1887731, 1887732, 1887733, 1887734, 1887735, 1887746, 1887747, 1887748 for 1, L¹, L², 2, L³, 3, 4, 5, 6, respectively) can be found in the Supporting Information or can be obtained free of charge from the Cambridge Crystallographic Data Centre via <https://summary.ccdc.cam.ac.uk/structure-summary-form>.

Electrospray Ionization Mass Spectrometry (ESI-MS). ESI-MS measurements were conducted at a capillary temperature of 275 °C. Aliquots of the solution were injected into the device at 0.3 mL/h. The mass spectrometer used for the measurements was a Thermo Exactive Plus, and the data were collected in positive and negative ion modes. The spectrometer was calibrated with the standard tune mix to give a precision of ca. 2 ppm in the region of 200–2000 m/z . The capillary voltage was 50 V, the tube lens voltage was 150 V, and the skimmer voltage was 25 V. The in-source energy was set to the range of 0–100 eV with a gas flow rate at 15% of the maximum. Preliminary ESI-MS has been used to probe the integrity and behaviour of the cluster in solution, and detection of trace intermediates of time dependent under photoexcitation. Due to the solubility limitation in CH₃CN, CH₃OH and H₂O, the crystals of them were dissolved in DMSO and diluted with CH₃OH for ESI-MS at 275 °C with positive mode.

Density Functional Theory Calculations. Density functional theory calculations were carried out using B3LYP/6-311g*, functional adding the D3 version of Grimme's dispersion with Becke-Johnson damping, SDD for Zn and 6-31+g basis sets for other elements using Gaussian 09 software.^[21] Bonding order were analyzed using Multiwfn software.^[22] The geometry of LZnCl₂ were fully optimized assuming C₄ symmetry, Mayer bond order was then calculated based on the optimized geometry. Attempt to calculate complexation energies of different possible fragments based on single-crystal geometry failed due to *scf* convergence problem.

Optical Properties. Emission and excitation spectra and emission lifetimes were measured using the same slit and iris. The solid-state quantum yields of powder samples in sealed quartz cuvettes and as films spin-coated on quartz substrates were measured using the integrating

sphere (142 mm in diameter) of Edinburgh FLS980 Spectro fluorophotometer (the ratio between signal to noise ca. 6000 : 1 by using the Raman peak of water) with the same slit (1.9980 mm) and iris (10, the largest one is 100 in our experiments).

Acknowledgements

This work was supported by the National Science Foundation for Distinguished Young Scholars of China (No. 21525101), NSF (No. 21571165), the NSF of Hubei Province innovation group project (2017CFA006), and the NSF of China and Guangxi Province (2014GXNSFFA118003, 2017GXNSFDA198040), the BAGUI talent and scholar program (2014A001), the Project of Talents Highland of Guangxi Province. MK is funded by the CNRS-France.

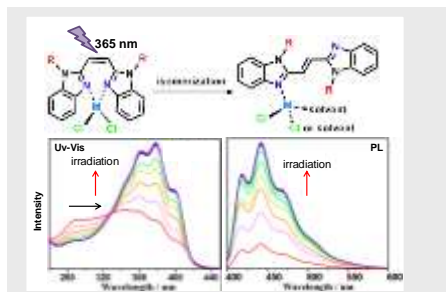
Keywords: *Trans / cis* conversion • Thermally or photo induced isomerization • Absorption and luminescence • Metal coordination • Steric substituent

- [1] Y. Kamiya, H. Asanuma, *Acc. Chem. Res.* **2014**, *47*, 1663–1672.
- [2] H. M. D. Bandara, S. C. Burdette, *Chem. Soc. Rev.* **2012**, *41*, 1809–1825.
- [3] a) X. Guo, J. Zhou, M. A. Siegler, A. E. Bragg, H. E. Katz, *Angew. Chem. Int. Ed.* **2015**, *54*, 4782–4786; *Angew. Chem.* **2015**, *127*, 4864–4868; b) H.-B. Xu, T. He, M.-J. Tang, X. Peng, J.-G. Deng, *Chin. Sci. Bull. (Chin Ver)* **2014**, *59*, 2900–2917.
- [4] a) J. Zhou, X. Guo, H. E. Katz, A. E. Bragg, *J. Am. Chem. Soc.* **2015**, *137*, 10841–10850; b) R. S. H. Liu, *Acc. Chem. Res.* **2001**, *34*, 555–562.
- [5] a) A. M. Caamaño, M. E. Vázquez, J. Martínez-Costas, L. Castedo, J. L. Mascareñas, *Angew. Chem. Int. Ed.* **2000**, *39*, 3104–3107; *Angew. Chem.* **2000**, *112*, 3234–3237; b) C.-S. Tsai, J.-K. Wang, R. T. Skodje, J.-C. Lin, *J. Am. Chem. Soc.*, **2005**, *127*, 10788–10789.
- [6] a) D. H. Waldeck, *Chem. Rev.* **1991**, *91*, 415–436; b) H. Petek, Y. Fujiwara, D. Kim, K. Yoshihara, *J. Am. Chem. Soc.* **1988**, *110*, 6269–6270.
- [7] H. Sugimoto, T. Kimura, S. Inoue, *J. Am. Chem. Soc.* **1999**, *121*, 2325–2326.
- [8] C. G. F. Cooper, J. C. MacDonald, E. Soto, W. G. McGimpsey, *J. Am. Chem. Soc.* **2004**, *126*, 1032–1033.
- [9] R. Lyndon, K. Konstas, B. P. Ladewig, P. D. Southon, C. J. Kepert, M. R. Hill, *Angew. Chem. Int. Ed.* **2013**, *125*, 3783–3786; *Angew. Chem.* **2013**, *125*, 3783–3786.
- [10] a) K. P. S. Zannoni, N. Y. M. Iha, *Dalton Trans.* **2017**, *46*, 9951–9958; b) W.-T. Sun, G. Huang, S.-J. Huang, Y. Lin, J. Yang, *J. Org. Chem.* **2014**, *79*, 6321–6325; c) L. M. L. Daku, J. Linares, M. Boillot, *Phys. Chem. Chem. Phys.* **2010**, *12*, 6107–6123.
- [11] J. M. Cameron, L. Vilà-Nadal, R. S. Winter, F. Iijima, J. C. Murillo, A. Rodríguez-Forteza, H. Oshio, J. M. Poblet, L. Cronin, *J. Am. Chem. Soc.* **2016**, *138*, 8765–8773.
- [12] a) D. Fujita, Y. Ueda, S. Sato, N. Mizuno, T. Kumasaka, M. Fujita, *Nature* **2016**, *540*, 563–566; b) K. Li, L.-Y. Zhang, C. Yan, S.-C. Wei, M. Pan, L. Zhang, C.-Y. Su, *J. Am. Chem. Soc.* **2014**, *136*, 4456–4459.
- [13] a) H. X. Na, P. Y. Yang, Z. Yin, Y. H. Wang, L. X. Chang, R. Si, M. Kurmoo, M. H. Zeng, *Chem. Eur. J.* **2016**, *22*, 18404–18411; b) Y. Q. Hu, M. H. Zeng, K. Zhang, S. Hu, F. F. Zhou, M. Kurmoo, *J. Am. Chem. Soc.* **2013**, *135*, 7901–7908.
- [14] a) M.-H. Zeng, Z. Yin, Z.-H. Liu, H.-B. Xu, Y.-C. Feng, Y.-Q. Hu, L.-X. Chang, Y.-X. Zhang, J. Huang, M. Kurmoo, *Angew. Chem. Int. Ed.* **2016**, *55*, 11407–11411; *Angew. Chem.* **2016**, *128*, 11579–11583; b) X.-L. Chen, H.-B. Xu, X.-X. Shi, Y. Zhang, T. Yang, M. Kurmoo, M.-H. Zeng, *Inorg. Chem.*, **2017**, *56*, 14069–14076.
- [15] J.-P. Zhong, B. Liu, T. Yang, Y.-J. Liu, Z.-H. Zhu, B.-F. Shi, M. Kurmoo, M.-H. Zeng, *Inorg. Chem.* **2017**, *56*, 10123–10126.
- [16] B. Liu, F. Yu, M. Tu, Z.-H. Zhu, Y.-X. Zhang, Z.-W. Ouyang, Z. Wang, M.-H. Zeng, *Angew. Chem. Int. Ed.* **2018**, DOI 10.1002/anie.201813829.
- [17] D. Zhang, S. Liu, X. Duan, Y. He, Y. Deng, *Inorg Nano-Metal Chem.*, **2017**, *47*, 1457–1461.
- [18] a) S. Poplata, A. Troster, Y.-Q. Zou, T. Bach, *Chem. Rev.* **2016**, *116*, 9748–9815; b) J. Vansant, S. Toppet, G. Smets, J. P. Declercq, G. Germain, M. V. Meerssche, *J. Org. Chem.* **1980**, *45*, 1565–1573.
- [19] a) G. M. Sheldrick, *Acta Cryst. A.* **2008**, *64*, 112–122; b) *Acta Cryst. C.* **2015**, *71*, 3–8.
- [20] M. Burgert, S. Voss, S. Herr, M. Fonin, U. Groth, U. Rudiger, *J. Am. Chem. Soc.* **2007**, *129*, 14362–14366.
- [21] M. J. Frisch, G. W. Trucks, H. B. Schlegel, et al. Gaussian 09; Gaussian, Inc.: Wallingford, CT, **2009**.
- [22] T. Lu, F. Chen, *J. Comput. Chem.* **2012**, *33*, 580–592.

Entry for the Table of Contents

FULL PAPER

Thermal treatment at 140 °C of *trans*-L in the presence of $M^{II}Cl_2$ (M = Fe, Co, Ni, Zn) led to stable (*cis*-L) MCl_2 and photoexcitation of the latter transform it back to (*trans*-L) MCl_2 (solvent). The kinetics can be followed using UV-Vis absorption and luminescence. The results are founded by further ESI-MS, NMR, and PXRD and DFT calculations.



Jun-Quan Zhang, De-Shan Zhang,
Qiu-Jie Chen, Hai-Bing Xu,*
Mohamedally Kurmoo, Ming-Hua Zeng*

Page No.1 – Page No.9

**Thermally-induced trans-to-cis
isomerization and its photo-induced
reversal monitored using absorption
and luminescence: Cooperative effect
of metal coordination and steric
substituent**